Journal of
Water & Climate Change

IWA PUBLISHING

Journal of Water and Climate Change Vol 13 No 2, 758 doi: 10.2166/wcc.2021.238

Hydrological impacts of climate and land-use change on flow regime variations in upper Indus basin

Kashif Haleem [a], Afed Ullah Khan [a,b,*], Sohail Ahmad[b], Mansoor Khan[b], Fayaz Ahmad Khan[a,b], Wisal Khan[b] and Jehanzeb Khan [c]

[a] National Institute of Urban Infrastructure Planning, University of Engineering and Technology, Peshawar, Peshawar 25000, Pakistan
[b] Department of Civil Engineering, University of Engineering and Technology Peshawar (Bannu Campus), 28100 Bannu, Pakistan
[c] Higher Education Department, Government Post Graduate College Kohat, KPK, Pakistan
*Corresponding author. E-mail: afedullah@uetpeshawar.edu.pk

KH, 0000-0002-3025-8593; AUK, 0000-0002-2742-0377; JK, 0000-0003-3517-2761

ABSTRACT

Investigating the effects of climate and land-use changes on surface runoff is critical for water resources management. The majority of studies focused on projected climate change effects on surface runoff, while neglecting future land-use change. Therefore, the main aim of this article is to discriminate the impacts of projected climate and land-use changes on surface runoff using the Soil and Water Assessment Tool (SWAT) through the lens of the Upper Indus Basin, Pakistan. Future scenarios of the land-use and climate changes are predicted using cellular automata artificial neural network and four bias-corrected general circulation models, respectively. The historical record (2000–2013) was divided into the calibration period (2000–2008) and the validation period (2009–2013). The simulated results demonstrated that the SWAT model performed well. The results obtained from 2000 to 2013 show that climate change (61.61%) has a higher influence on river runoff than land-use change (38.39%). Both climate and land-use changes are predicted to increase future runoff depth in this basin. The influence of climate change (12.76–25.92%) is greater than land-use change (0.37–1.1%). Global weather data has good applicability for simulating hydrological responses in the region where conventional gauges are unavailable. The study discusses that both climate and land-use changes impact runoff depth and concludes with some suggestions for water resources managers to bring water environment sustainability.

Key words: CA-ANN model, climate change, land-use change, runoff responses, SWAT model

HIGHLIGHTS

- The SWAT model was used to isolate the climate and land-use change impacts on streamflow.
- The general circulation model was used to assess climate change impacts on streamflow.
- The CA-ANN model was used to predict future land use.
- Multiple climate and land-use scenarios were set to isolate climate and land-use change impacts on streamflow.
- Climate change effects overweigh the land-use change effects on streamflow.

GRAPHICAL ABSTRACT

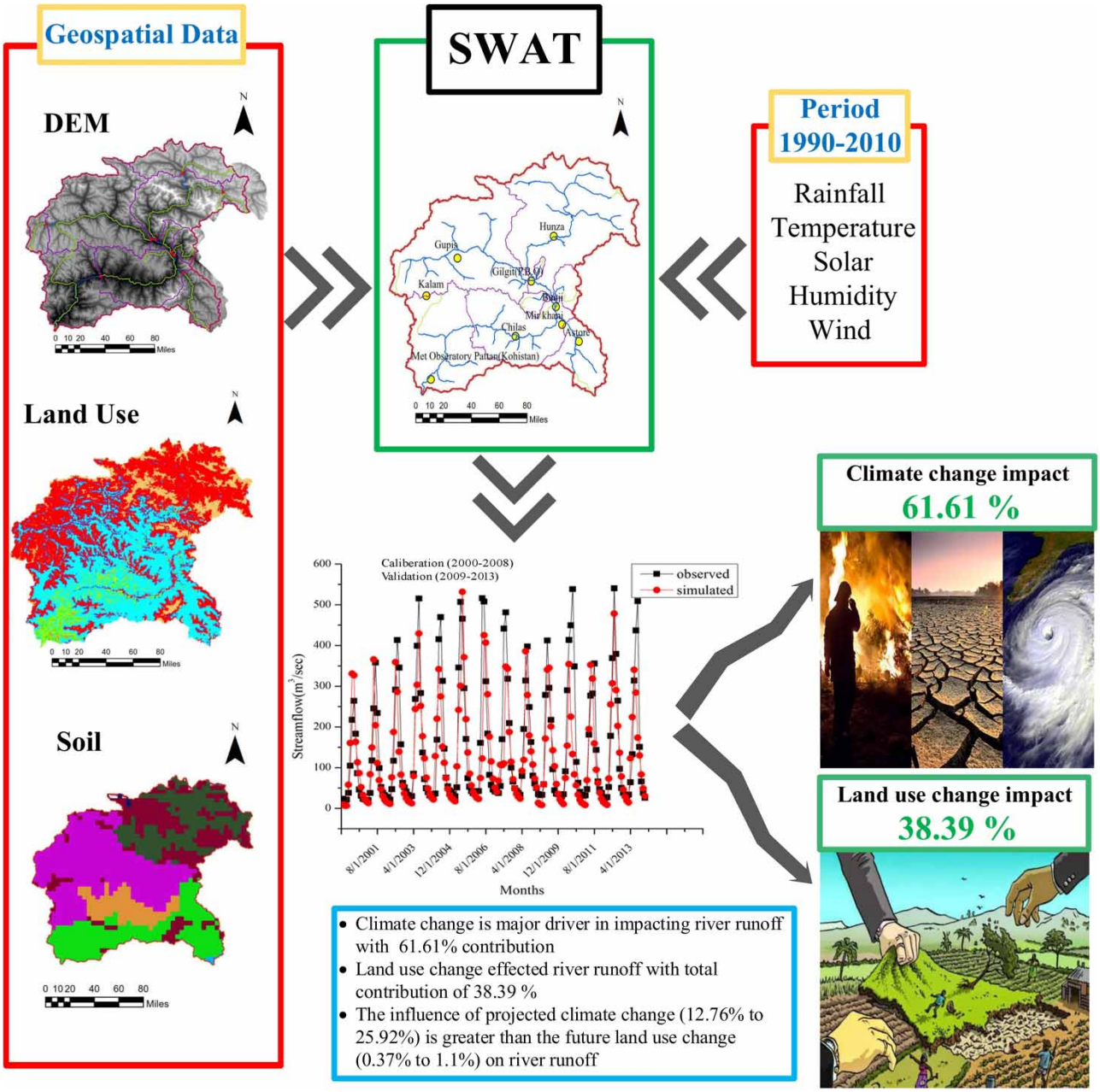

1. INTRODUCTION

Reduction in streamflow is the main concern in most of the river basins that supply water for agriculture, industry, and the growing population along the river (Zhang *et al.* 2017). The major concern of today's world is the global potential climate change impacts on water resources. It causes natural disasters, i.e. monsoonal flood hazards (Nanding *et al.* 2020), wildfire risk (Du *et al.* 2021), and severe drought (Pokhrel *et al.* 2021). This devastation is increased by changes in the watershed's land use (Stocker *et al.* 2001). Land-use and climate change have a major influence on water ecology, which are often reflected in long-term geographical and temporal changes in the water balance components, such as runoff, soil moisture, evapotranspiration, groundwater, and streamflow (Fang *et al.* 2013; Memarian *et al.* 2014; Deng *et al.* 2015). Runoff is the interface of climate and land-use change in a basin where climate change mostly affects the spatial distribution and temporal

variability of runoff. Land-use change refers to the human intervention on natural processes which badly impact river flow (Li *et al.* 2009; Liu *et al.* 2010; Wang *et al.* 2014; Birkinshaw *et al.* 2017; Zhang *et al.* 2017). Therefore, it is critical to quantify the impacts of climate and land-use changes on river runoff in order to assist policymakers and watershed managers in achieving watershed sustainability (Liu *et al.* 2010; Shang *et al.* 2019).

Pakistan is one of the world's water-stressed countries, with an annual average rainfall of 240 mm. Rapid urbanization and population increase are the major sources of water quality impairment at the basin scale (Ghoraba 2015). Previously, the water supply systems were built considering climatic trends that cause variations in streamflow. Variations in precipitation pose a great challenge to water resources management. These negative consequences of anthropogenic activities – both qualitatively and quantitively on water resources – restrict the use of water to meet the growing demands of future populations (Mukheibir 2007; Obuobie *et al.* 2012).

In this study, the watershed hydrological model, Soil and Water Assessment Tool (SWAT), incorporated in Geographic Information System (GIS) was applied. The SWAT model is frequently used nowadays because it is a river basin scale model capable of simulating the impacts of land management practices in large, complex watersheds, including the impacts that occur in the smaller modeling units, called hydrologic response units (HRUs). The SWAT has been termed by many studies as a computationally highly efficient model for forecasting the effects of land use and climate change on streamflow (Neitsch *et al.* 2011). Numerous studies have evaluated the SWAT model's effectiveness while globally assessing hydrological processes in various areas (Khan *et al.* 2014; Shang *et al.* 2019).

The Intergovernmental Panel on Climate Change (IPCC) has developed the most advanced numerical-based general circulation models (GCMs) to understand the future global climatic systems, such as the atmosphere, the sea ice, and the ocean (Fowler *et al.* 2007; Mahmood & Babel 2013). These models are very efficient in forecasting climate changes across the globe; but, outputs obtained from these models are completely based on large grid sizes that range from 250 to 600 km, which restrict its use in the evaluation of hydrological impacts caused by climate change (Wilby *et al.* 2000; Gebremeskel *et al.* 2004). However, dynamical and statistical downscaling (SD) methods have been developed to include GCM data into hydrological models to predict climate change. SD is often used by various institutions working on climate change (Wilby *et al.* 2000; Fowler *et al.* 2007).

While many researchers have investigated water quality problems in Pakistan (Daud *et al.* 2017; Bashir *et al.* 2020), there is a deficiency in evaluating the impacts of both land use and climate changes on a large and complex watershed scale. The main purpose of this study is to understand how surface runoff responds to projected land use and climate change at a representative watershed scale to provide a solid background for long-term water resource prediction and planning in the upper region of the Indus River. Moreover, this study also separates the impacts of climate and land-use change on river runoff.

2. STUDY AREA DESCRIPTION, DATA COLLECTION, AND METHODS

2.1. Study area description

The study area comprises the Indus River which is shared by Pakistan, China, Afghanistan, and India and covers a total area of 1.1×10^6 km^2 (Lutz *et al.* 2014). Moreover, the largest part of the Indus River basin lies in Pakistan and the smallest part in Afghanistan. It is extended between 32.48–37.07°N and 67.33–81.83°E (Archer 2003). This research study is confined to the upper region of the Indus River of Pakistan at Astore (Gilgit Baltistan) as shown in Figure 1, whose basin area is 45,400 km^2 and elevation range is from 547 to 8,060 m.

2.2. Data collection

This research study is based on the following datasets whose details are given below.

2.2.1. Digital elevation model

Digital elevation model (DEM) data of the study area has been downloaded from the National Aeronautics and Space Administration (NASA) (https://earthdata.nasa.gov/). The resolution of the Advanced Spaceborne Thermal Emission and Reflection Radiometer (ASTER) GDEM (Global Digital Elevation Model) is 30 m × 30 m. DEM data is used for watershed delineation. The delineated watershed is demonstrated in Figure 1.

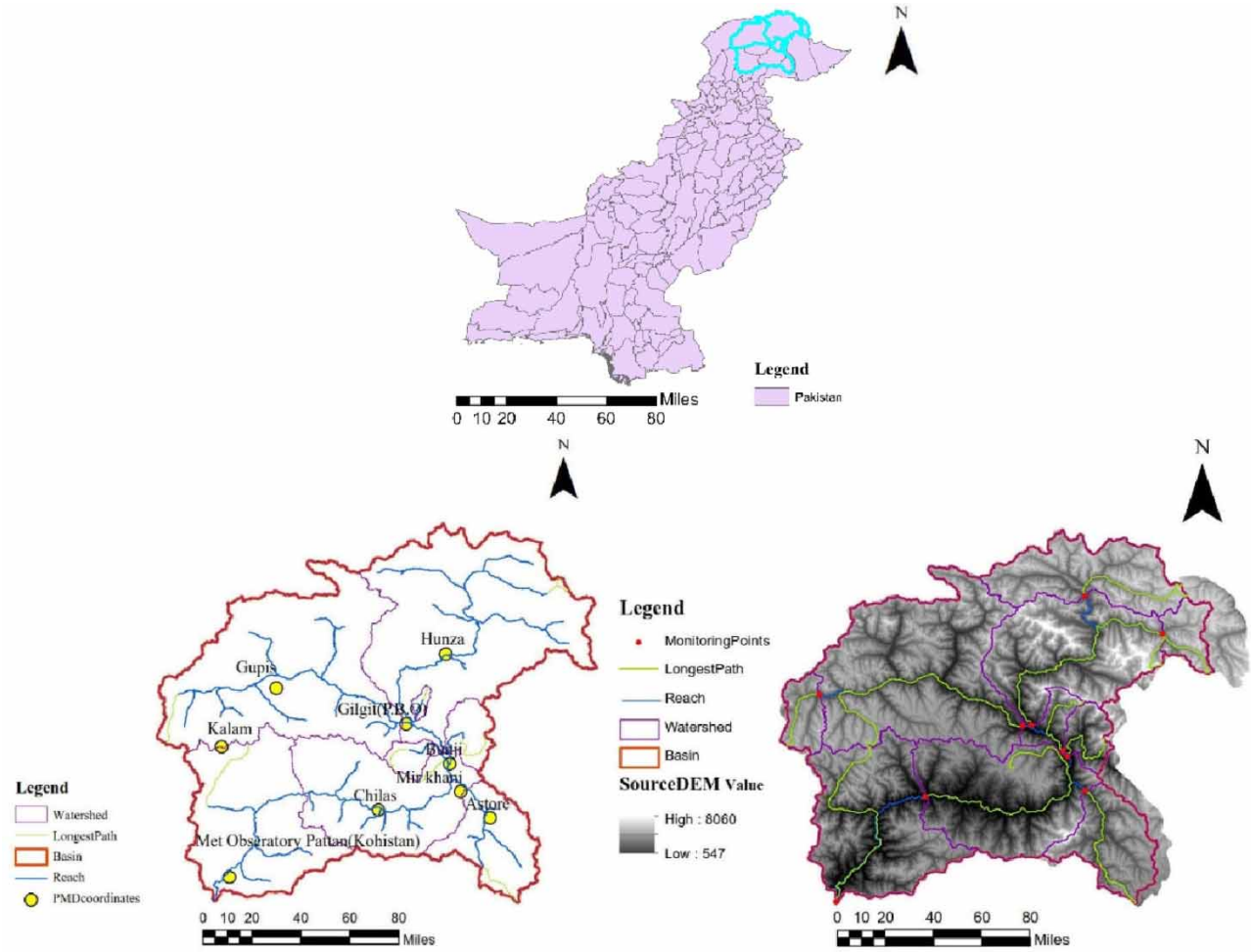

Figure 1 | Overview of study area showing the delineated watershed.

2.2.2. Land use

Land-use data of Moderate Resolution Imaging Spectroradiometer (MODIS) was downloaded from the United States Geological Survey (USGS) (https://earthexplorer.usgs.gov/). The details of land-use classes and their percentages composition for the delineated watershed are demonstrated in Figure 2.

2.2.3. Soil data

Soil data was downloaded from the Food and Agriculture Organization (FAO) (http://www.fao.org/). The details of soil classes and their percentage compositions for the delineated watershed are demonstrated in Figure 2.

2.2.4. Hydroclimatic data sets

Meteorological data, which includes precipitation, temperature (maximum and minimum), humidity, sunshine duration, evapotranspiration, and wind speed, were collected from Pakistan Meteorological Department (PMD) from 1990 to 2013. Similarly, hydrological data which includes daily and average flow were obtained from Water and Power Development Authority (WAPDA) for the period of 1990–2013. Our study area includes a total of nine PMD stations, in which only four stations' data are available. Because of the unavailability of meteorological data, Global Weather data was used for simulation purposes. The PMD coordinates and WAPDA monitoring stations are depicted in Figure 1.

Daily precipitation and temperature (min and max) of four GCMs, namely, GFDL-ESM2G, HadGEM2-ES, MIROC5, and CanESM2 were used for simulations in the SWAT model from 2005 to 2010, which were obtained from Coupled Model

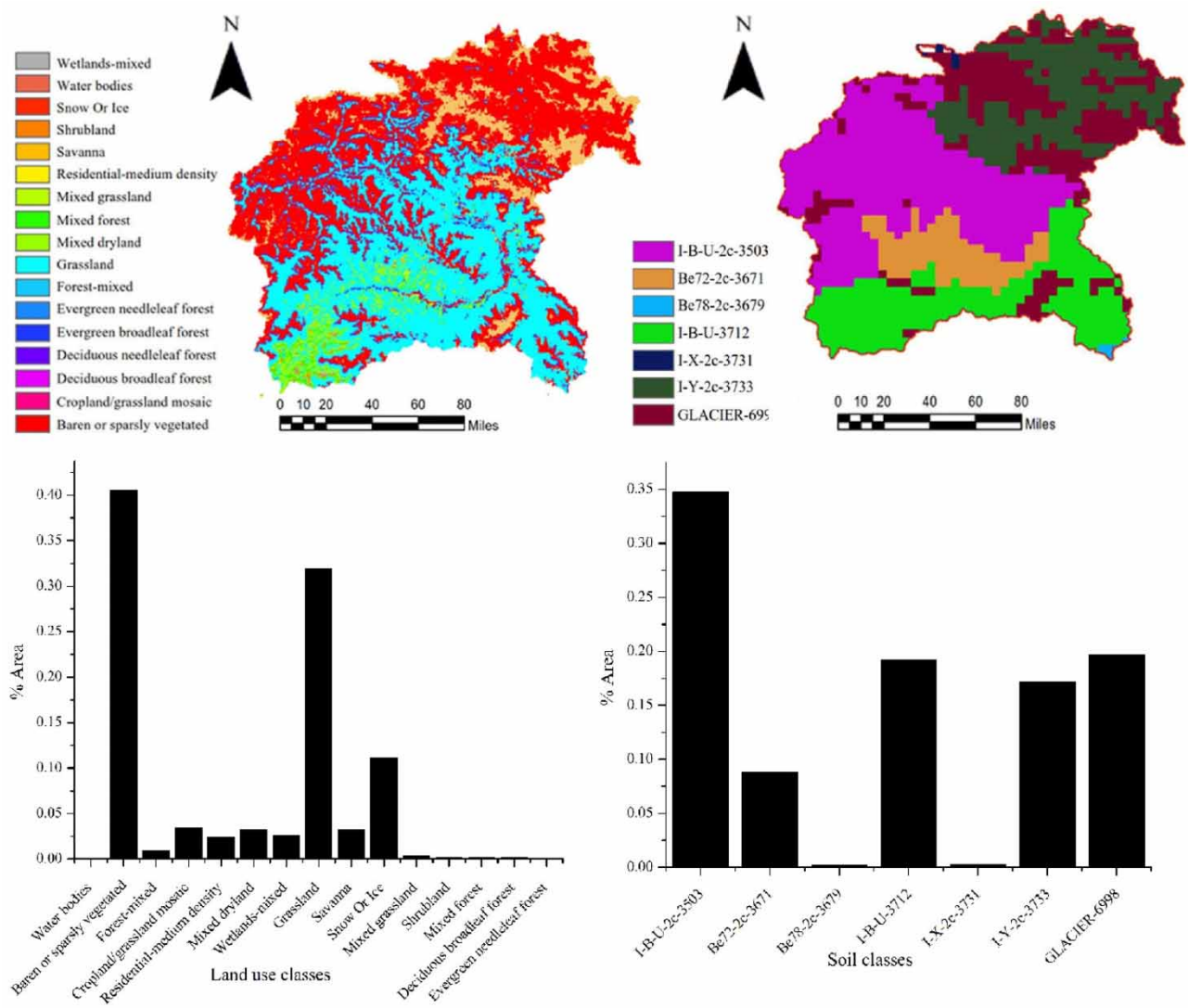

Figure 2 | Details of the land use and soil classes and their percentage compositions.

Intercom-parison Project Phase 5 (CMIP5) archive. These models are frequently used in the Asian region (Babar *et al.* 2015; Prasanna 2015; Mahmood & Jia 2016). The description of four GCMs is listed in Table 1.

2.3. Methods

2.3.1. Bias correction of GCMs

Bias corrections are often applied to climate models when they do not show any/little similitude to observed data. GCMs are corrected by bias corrections which use a transformation algorithm to relate outputs of GCMs. The main objective of the

Table 1 | Overview of the GCMs adopted for the current study

Modeling centre	Model	Institute ID	Resolution (km)
Geophysical Fluid Dynamics Laboratory, USA	GFDL-ESM2G	GFDL	90 × 144
Met Office Hadley Centre, UK	HadGEM2-ES	MOHC	145 × 192
Atmosphere and Ocean Research Institute, The University of Tokyo, Japan	MIROC5	MIROC	128 × 256
Canadian Centre for Climate Modelling and Analysis, Canada	CanESM2	CCCma	192 × 288

biases is to create a correlation between observed and simulated data, which will be the premise for correcting future projections of GCMs (Sun *et al.* 2011; Nguyen *et al.* 2020). The climate model data for hydrologic modeling (CMhyd) tool was used for biasing climate models (Rathjens *et al.* 2016b). There are plenty of biasing methods in the CMhyd tool, i.e. linear scaling (additive and multiplicative), delta change correction (additive and multiplicative), power transformation of precipitation, precipitation local intensity scaling, variance scaling of temperature, and distribution mapping of precipitation and temperature (Rathjens *et al.* 2016a). Utilizing GCM results at the regional scale is more straightforward and faster with linear scaling than with statistical or dynamic downscaling. These methods are used to correct biases in GCM or RCM findings. SD involves the development of empirical relationships between local-scale variables (e.g. temperature or precipitation) and large-scale variables (e.g. specific humidity, sea level pressure, and temperature of GCMs), and then simulating future data using these relationships. However, bias correction successfully corrects the simulated GCM results (e.g. temperature and precipitation) (Fang *et al.* 2015). We have used linear scaling (additive and multiplicative) bias correction for our study area (Worku *et al.* 2020).

2.3.2. Description of SWAT model

The SWAT model is a watershed hydrological model incorporated in the GIS developed by the United States Department of Agriculture in the 1990s. It was designed to predict the effects of weather, different land-use patterns, and soil conditions on river runoff (Yi & Sophocleous 2011; Yu *et al.* 2013; Wisal *et al.* 2020). The SWAT model requires topographic (DEM), land-use/land-cover, soil, and daily weather (precipitation and temperature) data as their minimum inputs (Ficklin & Barnhart, 2014). The SWAT model uses water balance equation for simulation as follows:

$$\mathrm{SW_t} = \mathrm{SW_o} + \sum_{i=o}^{t} (R_{\mathrm{day}} - Q_{\mathrm{surf}} - E_{\mathrm{a}} - W_{\mathrm{seep}} - Q_{\mathrm{gw}})_i \quad (1)$$

where $\mathrm{SW_t}$ is the final soil moisture content, mm; $\mathrm{SW_0}$ is the initial soil moisture content of the ith day, mm; t is the time, d; R_{day} is the precipitation of the ith day, mm; Q_{surf} is the surface runoff of day i, mm; E_{a} indicates the amount of evapotranspiration on day i, mm; W_{seep} indicates the amount of water entering the vale zone from the soil profile on day i, mm; and Q_{gw} indicates the return flow amount on day i, mm.

2.3.3. SWAT model calibration and validation

The Doyian station at Astore River was selected for model calibration to evaluate the dominant parameters of the streamflow using SWAT-CUP (SWAT Calibration and Uncertainty Procedures) automatic calibration with the Sequential Uncertainty Fitting program algorithm (SUFI-2) (Shang *et al.* 2019). The SWAT-CUP model was calibrated using monthly data from 2000 to 2008. Calibration is a process to assess the goodness of fit between the observed and simulated data to get the optimum values of representative functions such as Nash–Sutcliffe efficiency (NSE), coefficient of determination (R^2), root-mean-square error to the standard deviation ratio (RSR), and percent bias (PBIAS). For RSR and PBIAS, the most optimum value is zero, whereas for R^2 and NSE, it is 1. The R^2 value ranges from 0 to 1; values closer to 1 indicate the best results, while greater than 0.5 is in an acceptable range. Succeeding calibration, the model was validated for monthly data from 2009 to 2013. The model efficiency was tested in the validated period by evaluating the decision factors as shown in Table 2.

Table 2 | Statistical indicators for model performance evaluation

Performance rating	NSE	RSR	PBIAS (%)
Very good	$0.75 < \mathrm{NSE} \leq 1$	$0 \leq \mathrm{RSR} \leq 0.5$	$-10 < \mathrm{PBIAS} < 10$
Good	$0.65 < \mathrm{NSE} \leq 0.75$	$0.5 < \mathrm{RSR} \leq 0.6$	$\pm 10 \leq \mathrm{PBIAS} < \pm 15$
Satisfactory	$0.5 < \mathrm{NSE} \leq 0.65$	$0.6 < \mathrm{RSR} \leq 0.7$	$\pm 15 \leq \mathrm{PBIAS} < \pm 25$
Unsatisfactory	$\mathrm{NSE} \leq 0.5$	$\mathrm{RSR} > 0.7$	$\mathrm{PBIAS} \geq 25$

2.3.4. Climate and land-use change contribution rate assessment

The SWAT model was used to separate the percentage of climate change impacts from land use on river flow. The observed and simulated flow data were compared using preset climate and land-use scenarios. For instance, four scenarios were used in which scenario 1 and scenario 3 encountered the land-use change impacts on river runoff, while scenario 2 and scenario 4 encountered the climate change impacts on river runoff as given in Table 3. The contribution rate was computed by Equations (6) and (7) where Q_1, Q_2, Q_3, and Q_4 are the average river runoff obtained from the below-mentioned scenarios (Guo *et al.* 2016; Shang *et al.* 2019):

$$\Delta Q_C = Q_2 - Q_1 \tag{2}$$

$$\Delta Q_L = Q_3 - Q_1 \tag{3}$$

$$\Delta Q_M = Q_L + Q_C \tag{4}$$

$$\Delta Q = Q_4 - Q_1 \tag{5}$$

Hypothetically, ΔQ is equal to ΔQ_M, and thereafter, the impact of climate and land-use change on river runoff can be computed by η_C climate change and η_L land-use change:

$$\eta_C = \frac{\Delta Q_C}{\Delta Q_M} \times 100\% \tag{6}$$

$$\eta_L = \frac{\Delta Q_L}{\Delta Q_M} \times 100\% \tag{7}$$

2.3.5. Future land-use prediction

Land use was predicted for 2050 for the upper region of Indus River using the cellular automata artificial neural network (CA-ANN) model that uses QGIS plugin Modules for Land Use Change Simulations (MOLUSCE). Slope and aspects variables were used as land-use drivers. At the very outset, to check the model efficiency, the land use of 2001 and 2010 were used to predict the land use of 2015, and then that of 2050.

3. RESULTS AND DISCUSSION

3.1. Model calibration and validation

Calibration (2000–2008) and validation (2009–2013) were carried out on the observed flow data obtained from WAPDA at the Doyain outlet station at Astore River. A warm-up period of 2 years (1998–2000) was used to initialize the calibration process. The model calibration process was followed by sensitivity analysis to choose parameters that govern the observed river runoff. A total of 24 most effective parameters were selected for model calibration as demonstrated in Table 4. The model performance was evaluated to predict the watershed conditions by statistical indicators such as R^2, NSE, PBIAS, and RSR as given in Table 5, and simulated flow results are demonstrated in Figure 3.

3.2. Impacts of climate and land-use change on river runoff

The simulated annual streamflow results show the effects of climate and land-use change on river runoff over the preset scenarios as demonstrated in Table 6. The total variation observed in streamflow is 121.32 m^3/s. In the aforementioned total

Table 3 | Scenarios-based contribution rate analysis

Scenarios	Land use	Meteorological data
1	2001	2000–2008
2	2001	2008–2013
3	2013	2000–2008
4	2013	2008–2013

Table 4 | Parameters sensitive to river runoff, their fitted values, and initial ranges

Parameter	Description	Fitted value	Ranges
CN2.mgt	SCS runoff curve number	78.5	(35,98)
ALPHA_BF.gw	Baseflow alpha factor (days)	0.63	(0,1)
GW_DELAY.gw	Groundwater delay (days)	485.40	(0,500)
GWQMN.gw	Threshold depth of water in the shallow aquifer required for return flow to occur (mm)	534.95	(0, 5,000)
SURLAG.hru	Surface runoff lag time	12.52	(0.05,24)
SLSOIL.hru	Slope length for lateral subsurface flow	131.25	(0,150)
EPCO.hru	Plant uptake compensation factor	0.47	(0,1)
SOL_K(..).sol	Saturated hydraulic conductivity	283.33	(0, 2,000)
OL_AWC(..).sol	Available water capacity of the soil layer	0.52	(0,1)
CH_N2.rte	Manning's *n* value for the main channel	0.30	(−0.01,0.3)
SFTMP.bsn	Snowfall temperature	−4.56	(−20,20)
SMTMP.bsn	Snow melt base temperature	5.33	(−20,20)
SMFMX.bsn	Maximum melt rate for snow during year (occurs on summer solstice)	3.55	(0,20)
SMFMN.bsn	Minimum melt rate for snow during the year (occurs on winter solstice)	19.50	(0,20)
SNO50COV.bsn	Snow water equivalent that corresponds to 50% snow cover	0.25	(0,1)
CH_K2.rte	Effective hydraulic conductivity in main channel alluvium	481.32	(−0.01,500)
ESCO.hru	Soil evaporation compensation factor	0.60	(0,1)
OV_N.hru	Manning's *n* value for overland flow	17.45	(0.01,30)
LAT_TTIME.hru	Lateral flow travel time	49.07	(0,180)
CANMX.hru	Maximum canopy storage	97.50	(0,100)
CNOP{..}.mgt	SCS runoff curve number for moisture condition	29.13	(0,100)
RFINC(..).sub	Rainfall adjustment	63.25	(0,100)
TMPINC(..).sub	Temperature adjustment	64.98	(0,100)
SNO_SUB.sub	Initial snow water content	69.47	(0,150)

Table 5 | Statistical indicators for model calibration and validation which regulate the flow regime

Calibration (2000–2008)				Validation (2009–2013)			
R^2	NSE	PBIAS	RSR	R^2	NSE	PBIAS	RSR
0.7	0.69	9.7	0.56	0.66	0.61	21.3	0.62

variation in streamflow, climate and land-use changes contributed 74.75 and 46.58 m^3/s increase in the streamflow. Climate and land-use change caused 61.61 and 38.39% variations in the streamflow, respectively, in the upper region of the Indus River. It shows that climate change is the major driver in the understudy area which caused variation in the streamflow.

Climate and land-use changes significantly alter the hydrological cycle. Adaptation methods for water management should consider how climatic variability will impact the hydrological regime and water supplies (Krysanova & White 2015). Tan *et al.* (2015) used the SWAT model to investigate the effects of land-use change and climatic variability in the Johor River basin, Malaysia where temperature and precipitation showed a significant increasing trend. The results demonstrated that the anticipated climatic variability showed a greater impact on streamflow and evaporation, in comparison to the projected land-use changes.

3.3. Climatic effects on streamflow

The SWAT model was used to assess the influence of climate change, i.e. precipitation and temperature (min and max) on the streamflow using four different GCMs. The analysis was carried out for four different periods (2007–2020, 2021–2034, 2035–

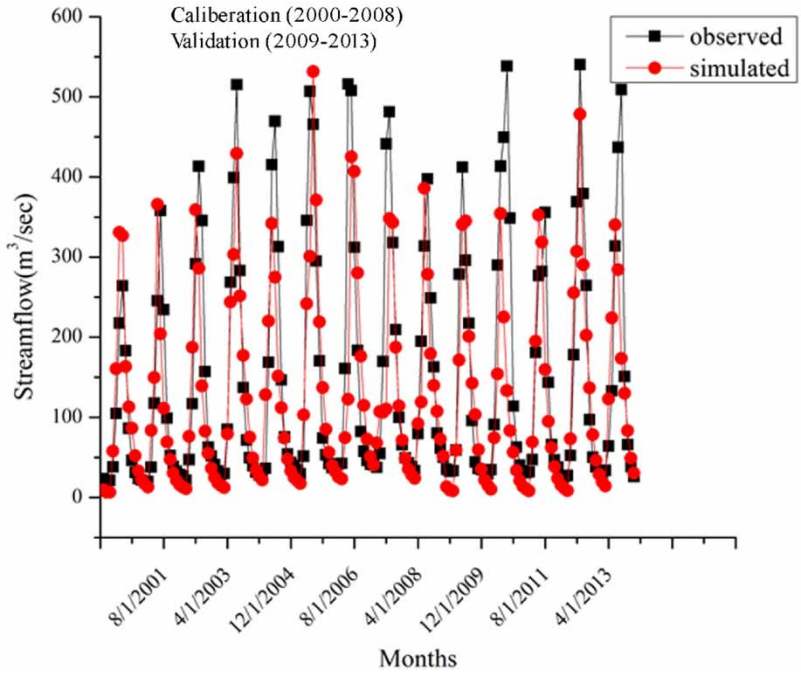

Figure 3 | SWAT model monthly streamflow calibration and validation results.

Table 6 | Climate and land use change impacts on streamflow under different scenarios

Scenarios	Period	Simulated annual runoff (m^3/s)	Variation (m^3/s)	% Climate contribution	% Land-use contribution
1	2000–2008	94.48	0		
2	2009–2013	151.23	56.75	61.61	38.39
3	2000–2008	129.84	35.36		
4	2009–2013	123.69	29.21		

2048, and 2086–2099). Table 7 shows the future mean annual streamflow of four GCMs at Astore River, Doyian station where a remarkable increase was observed in future streamflow in comparison to its base period (2007–2020).

Neupane *et al.* (2014) investigated the impacts of climate change on monsoon-driven streamflow in a central Himalayan watershed where predicted streamflow increased during the monsoon and post-monsoon seasons, while decreasing during the pre-monsoon season. Sood *et al.* (2013) used the SWAT model to assess the climate change impacts on the Volta River Basin in West Africa, where rainfall showed a decreasing trend while air temperature exhibited an increasing trend causing greater variability and reduced (40%) streamflow.

3.4. Land-use change effects on streamflow

Land use for the year 2050 was projected using QGIS plugin MOLUSCE. First, the land use of 2001 and 2010 was used to predict the land use of 2015, using CA-ANN. Later, the projected land-use map of 2015 was compared with NASA MODIS

Table 7 | Future prediction of streamflow (m^3/s) based on the four GCM models in the upper region of Indus River basin

Model	2007–2020	2021–2034	2035–2048	2086–2099
CanESM2	154.98	174.75 (+12.76%)	195.15 (+25.92%)	189.14 (+22.04%)
GFDL-ESM2G	150.12	178.25 (+18.74%)	183.36 (+22.14%)	173.47 (+15.55)
MIROC5	154.61	177.48 (+14.79%)	187.61 (+21.34%)	181.2 (+17.2%)
HadGEM2	158.69	184.45 (+16.23%)	193.85 (+22.16%)	186.77 (+17.7%)

land use for correctness and kappa value, which were found to be 80.26 and 0.72%, respectively. After validation, the land use of 2001 and 2018 was used to predict the land use of 2050. Increase and decrease are observed in different land-use classes as demonstrated. Figure 4 and Table 8 depict the area in percentages of variant land-use classes in different years.

Later, the projected land use of 2050 influence was evaluated on surface runoff using the SWAT model. The results showed that streamflow changes from 0.37 to 1.1% in response to the land use of 2018 and 2050.

The impacts of land-use/land-cover changes are evaluated using present trends and future scenarios. Getachew & Melesse (2012) studied the impacts of land-use change on the Angered watershed in Ethiopia. Decades of land-cover change affect runoff and reservoir inflow. Agricultural and urban areas increased, whereas forest and grassland areas shrank, affecting the mean monthly flow. Baker & Miller (2013) used the SWAT model to investigate how land development affects water resources in Kenya's River Njor. The results showed that dramatic alterations in land use have increased surface runoff and decreased groundwater recharge. Urbanization, agriculture, energy demand, and crop production are expected to grow in the Cedar River Basin of the Midwest, which will increase surface runoff and decrease baseflow (Wu *et al.* 2013). Schilling *et al.* (2014) examined the impacts of agricultural land use on flood risk reduction in Iowa's Raccoon River watershed. The study results unveiled that cropland conversion to permanent vegetation reduces the frequency of floods, but not their duration.

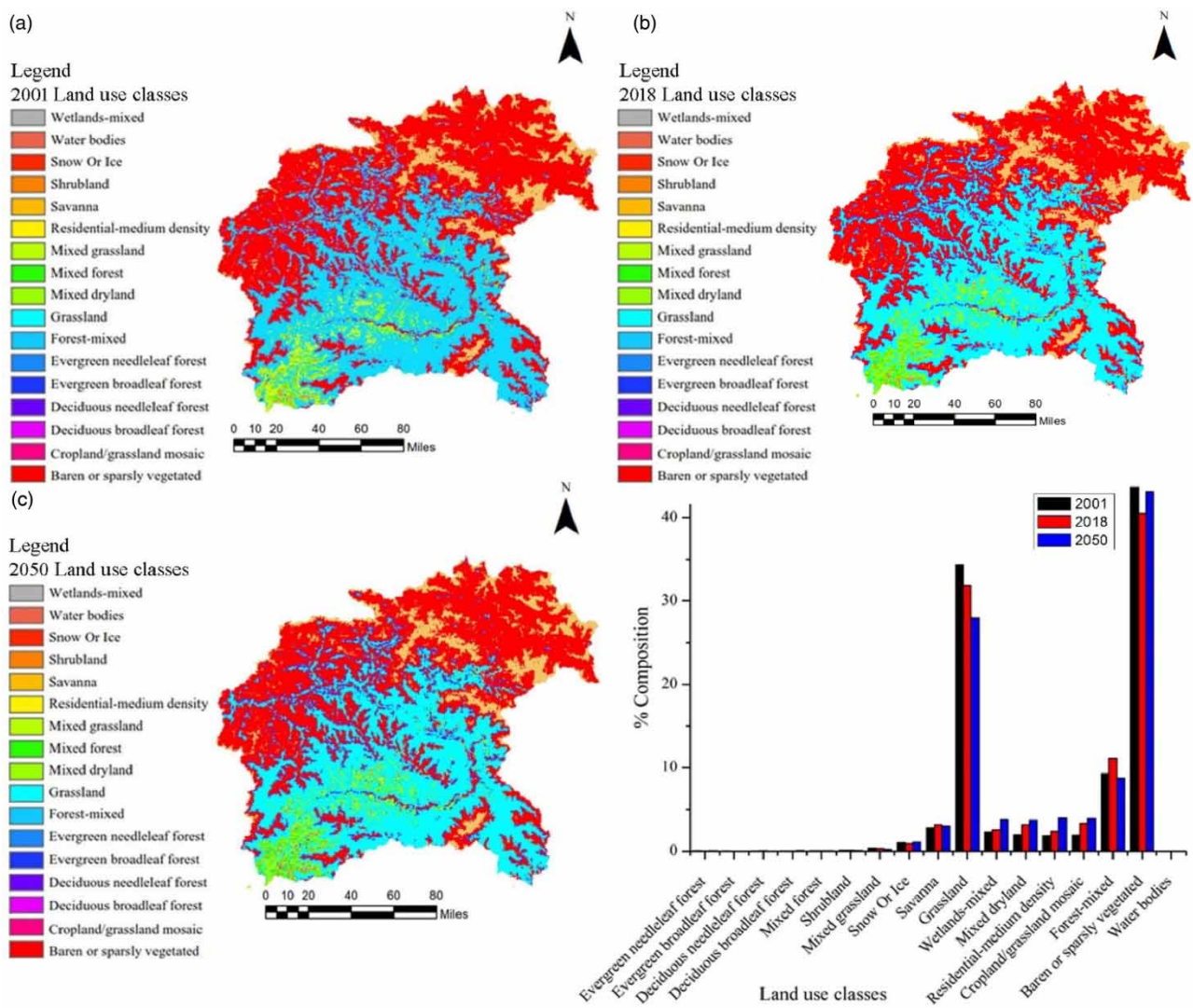

Figure 4 | Land-use maps of the study area: (a) 2001 land use, (b) 2018 land use, and (c) the predicted land use of 2050.

Table 8 | Area (%) change of different land-use classes

Land-use class	2001	2018	2050
Evergreen needleleaf forest	0.09%	0.05%	0.08%
Evergreen broadleaf forest	0.05%	0.03%	0.01%
Deciduous needleleaf forest	0.05%	0.08%	0.02%
Deciduous broadleaf forest	0.06%	0.04%	0.12%
Mixed forest	0.09%	0.09%	0.07%
Shrubland	0.14%	0.13%	0.12%
Mixed grassland	0.41%	0.35%	0.25%
Snow or ice	1.00%	0.90%	1.06%
Savanna	2.83%	3.19%	3.04%
Grassland	34.34%	31.90%	27.99%
Wetlands-mixed	2.31%	2.57%	3.77%
Mixed dryland	1.94%	3.20%	3.69%
Residential-medium density	1.86%	2.38%	3.96%
Cropland/grassland mosaic	1.88%	3.37%	3.89%
Forest-mixed	9.31%	11.13%	8.77%
Barren or sparsely vegetated	43.65%	40.55%	43.12%
Water bodies	0.02%	0.03%	0.03%

3.5. Watershed management implications

This study reported that climate change influence on the Indus flow regime overweighs land-use change. Climate change will increase water availability in the short term and decrease it in the long term. This dramatic change in flow regime is attributed to global warming. In the early 21st century, flow is expected to increase in summer followed by a decrease in the same in the late decades of the century. Summer and late spring discharges will increase in the short term because of excessive snowmelt, and in contrast, will decrease in the long term because of the disappearance of glaciers; but their effect will be lessened by rainfall. Some current aspects need re-assessment to improve waters condition in the basin. The sustainability of the current water system in the basin is questionable. Water management practices are suggested to store water which will help to lessen the influences of extreme conditions, i.e. flood and drought. The stored water will be used in the dry season for agriculture, hydropower, industrial, and domestic purposes. Furthermore, plantations are suggested in the study area to decline the increasing trend of air temperature as the sensitivity of streamflow is higher in the study area (Ahmad *et al.* 2020; Shah *et al.* 2021).

4. CONCLUSIONS

In this study, the SWAT model was used to evaluate the impacts of climate and land-use change on river runoff in the upper region of the Indus river basin. Future land-use and climate change scenarios are projected through the CA-ANN model and four bias-corrected GCM models, respectively. This study reported the percentage contribution of climate and land-use changes on runoff depth for the adopted as well as projected scenarios. The conclusions can be summarized as follows:

(1) The simulated results demonstrated that the SWAT model yields good statistical results during calibration (NSE = 0.69, R^2 = 0.7, RSR = 0.56, and PBIAS = 9.7) and validation (NSE = 0.61, R^2 = 0.66, RSR = 0.62, and PBIAS = 21.3).
(2) SWAT model was used to isolate the climate and land-use change impacts on river runoff in the upper region of the Indus river basin, Doyain station at Astore River, where the contribution rate of climate and land-use changes on surface runoff was 61.61 and 38.39%, respectively.
(3) GCMs (CanESM2, GFDL-ESM2G, MIROC5, and HadGEM2) based on CMIP5 have good applicability in the study area for the assessment of future climate change. Simulations with the calibrated model were conducted for 2007–2020, 2021–2034, 2035–2048, and 2086–2099 periods, where an increase was observed in the average annual river runoff.
(4) The predicted land use of 2050 by the CA-ANN model indicated an increasing trend of river runoff in the future by 1.1%.

DATA AVAILABILITY STATEMENT

All relevant data are included in the paper or its Supplementary Information.

REFERENCES

Ahmad, W., Khan, A. U., Khan, F. A., Farooq, M., Baig, A. A., Shah, L. A. & Khan, J. 2020 How vegetation spatially alters the response of precipitation and air temperature? Evidence from Pakistan. *Asian J. Atmos. Environ.* **14** (2), 133–145.

Archer, D. 2003 Contrasting hydrological regimes in the upper Indus Basin. *J. Hydrol.* **274**, 198–210.

Babar, Z. A., Zhi, X.-f. & Fei, G. 2015 Precipitation assessment of Indian summer monsoon based on CMIP5 climate simulations. *Arab. J. Geosci.* **8**, 4379–4392.

Baker, T. J. & Miller, S. N. 2013 Using the Soil and Water Assessment Tool (SWAT) to assess land use impact on water resources in an East African watershed. *J. Hydrol.* **486**, 100–111.

Bashir, N., Saeed, R., Afzaal, M., Ahmad, A., Muhammad, N., Iqbal, J., Khan, A., Maqbool, Y. & Hameed, S. 2020 Water quality assessment of lower Jhelum canal in Pakistan by using geographic information system (GIS). *Groundwater for Sustainable Development* **10**, 100357.

Birkinshaw, S. J., Guerreiro, S. B., Nicholson, A., Liang, Q., Quinn, P., Zhang, L., He, B., Yin, J. & Fowler, H. J. 2017 *Climate Change Impacts on Yangtze River Discharge at the Three Gorges Dam*.

Daud, M., Nafees, M., Ali, S., Rizwan, M., Bajwa, R. A., Shakoor, M. B., Arshad, M. U., Chatha, S. A. S., Deeba, F. & Murad, W. 2017 Drinking water quality status and contamination in Pakistan. *BioMed research international* **2017**, 7908183.

Deng, Z., Zhang, X., Li, D. & Pan, G. 2015 Simulation of land use/land cover change and its effects on the hydrological characteristics of the upper reaches of the Hanjiang Basin. *Environ. Earth Sci.* **73**, 1119–1132.

Du, J., Wang, K. & Cui, B. 2021 Attribution of the extreme drought-related risk of wildfires in spring 2019 over Southwest China. *Bulletin of the American Meteorological Society* **102** (1), S83–S90.

Fang, X., Ren, L., Li, Q., Zhu, Q., Shi, P. & Zhu, Y. 2013 Hydrologic response to land use and land cover changes within the context of catchment-scale spatial information. *J. Hydrol. Eng.* **18**, 1539–1548.

Fang, G., Yang, J., Chen, Y. & Zammit, C. 2015 Comparing bias correction methods in downscaling meteorological variables for a hydrologic impact study in an arid area in China. *Hydrology and Earth System Sciences* **19** (6), 2547–2559.

Ficklin, D. L. & Barnhart, B. L. 2014 SWAT hydrologic model parameter uncertainty and its implications for hydroclimatic projections in snowmelt-dependent watersheds. *Journal of hydrology* **519**, 2081–2090.

Fowler, H. J., Blenkinsop, S. & Tebaldi, C. 2007 Linking climate change modelling to impacts studies: recent advances in downscaling techniques for hydrological modelling. *Int. J. Climatol.* **27**, 1547–1578.

Gebremeskel, S., Liu, Y. B., De Smedt, F., Hoffmann, L. & Pfister, L. 2004 Analysing the effect of climate changes on streamflow using statistically downscaled GCM scenarios. *Int. J. River Basin Manag.* **2**, 271–280.

Getachew, H. E. & Melesse, A. M. 2012 The impact of land use change on the hydrology of the Angereb Watershed, Ethiopia. *Int. J. Water Sci.* **1** (6).

Ghoraba, S. M. 2015 Hydrological modeling of the Simly Dam watershed (Pakistan) using GIS and SWAT model. *Alex. Eng. J.* **54**, 583–594.

Guo, J., Su, X., Singh, V. P. & Jin, J. 2016 Impacts of climate and land use/cover change on streamflow using SWAT and a separation method for the Xiying River Basin in northwestern China. *Water* **8**, 192.

Khan, A., Ghoraba, S., Arnold, J. G. & Di Luzio, M. 2014 Hydrological modeling of upper Indus Basin and assessment of deltaic ecology. *Int. J. Mod. Eng. Res.* **4**, 73–85.

Krysanova, V. & White, M. 2015 Advances in water resources assessment with SWAT–an overview. *Hydrological Sciences Journal* **60** (5), 771–783.

Li, Z., Liu, W.-z., Zhang, X.-c. & Zheng, F.-l. 2009 Impacts of land use change and climate variability on hydrology in an agricultural catchment on the Loess Plateau of China. *J. Hydrol.* **377**, 35–42.

Liu, D., Chen, X., Lian, Y. & Lou, Z. 2010 Impacts of climate change and human activities on surface runoff in the Dongjiang River basin of China. *Hydrol. Process.* **24**, 1487–1495.

Lutz, A., Immerzeel, W., Shrestha, A. & Bierkens, M. 2014 Consistent increase in High Asia's runoff due to increasing glacier melt and precipitation. *Nat. Clim. Change* **4**, 587–592.

Mahmood, R. & Babel, M. S. 2013 Evaluation of SDSM developed by annual and monthly sub-models for downscaling temperature and precipitation in the Jhelum basin, Pakistan and India. *Theor. Appl. Climatol.* **113**, 27–44.

Mahmood, R. & Jia, S. 2016 Assessment of impacts of climate change on the water resources of the transboundary Jhelum River basin of Pakistan and India. *Water* **8**, 246.

Memarian, H., Balasundram, S. K., Abbaspour, K. C., Talib, J. B., Boon Sung, C. T. & Sood, A. M. 2014 SWAT-based hydrological modelling of tropical land-use scenarios. *Hydrol. Sci. J.* **59**, 1808–1829.

Mukheibir, P. 2007 *Access to Water – the Impact of Climate Change in Small Municipalities*.

Nanding, N., Chen, Y., Wu, H., Dong, B., Tian, F., Lott, F. C., Tett, S. F., Rico-Ramirez, M. A., Chen, Y. & Huang, Z. 2020 Anthropogenic influences on 2019 July precipitation extremes over the mid–lower reaches of the Yangtze River. *Frontiers in Environmental Science* **8**, 230.

Neitsch, S. L., Arnold, J. G., Kiniry, J. R. & Williams, J. R. 2011 *Soil and Water Assessment Tool Theoretical Documentation Version 2009*. Texas Water Resources Institute, College Station, TX.

Neupane, R. P., Yao, J. & White, J. D. 2014 Estimating the effects of climate change on the intensification of monsoonal-driven stream discharge in a Himalayan watershed. *Hydrol. Process.* **28** (26), 6236–6250.

Nguyen, H., Mehrotra, R. & Sharma, A. 2020 Assessment of climate change impacts on reservoir storage reliability, resilience, and vulnerability using a multivariate frequency bias correction approach. *Water Resour. Res.* **56**, e2019WR026022.

Obuobie, E., Kankam-Yeboah, K., Amisigo, B., Opoku-Ankomah, Y. & Ofori, D. 2012 Assessment of water stress in river basins in Ghana. *J. Water Clim. Change* **3**, 276–286.

Pokhrel, Y., Felfelani, F., Satoh, Y., Boulange, J., Burek, P., Gädeke, A., Gerten, D., Gosling, S. N., Grillakis, M. & Gudmundsson, L. 2021 Global terrestrial water storage and drought severity under climate change. *Nature Climate Change* **11** (3), 226–233.

Prasanna, V. 2015 Regional climate change scenarios over South Asia in the CMIP5 coupled climate model simulations. *Meteorol. Atmos. Phys.* **12**, 561–578.

Rathjens, H., Bieger, K., Srinivasan, R., Chaubey, I. & Arnold, J. 2016a *CMhyd User Manual*. Texas A&M University, College Station, TX.

Rathjens, H., Bieger, K., Srinivasan, R., Chaubey, I. & Arnold, J. 2016b *CMhyd User Manual: Documentation for Preparing Simulated Climate Change Data for Hydrologic Impact Studies*. Texas A&M University, College Station, TX.

Schilling, K. E., Gassman, P. W., Kling, C. L., Campbell, T., Jha, M. K., Wolter, C. F. & Arnold, J. G. 2014 The potential for agricultural land use change to reduce flood risk in a large watershed. *Hydrol. Process.* **28** (8), 3314–3325.

Shah, L. A., Khan, A. U., Khan, F. A., Khan, Z., Rauf, A. U., Rahman, S. U., Iqbal, M. J., Ahmad, I. & Abbas, A. 2021 Statistical significance assessment of streamflow elasticity of major rivers. *Civil Eng. J.* **7** (5), 893–905.

Shang, X., Jiang, X., Jia, R. & Wei, C. 2019 Land use and climate change effects on surface runoff variations in the Upper Heihe River Basin. *Water* **11**, 344.

Sood, A., Muthuwatta, L. & McCartney, M. 2013 A SWAT evaluation of the effect of climate change on the hydrology of the Volta River basin. *Water Int.* **38** (3), 297–311.

Stocker, T., Clarke, G., Le Treut, H., Lindzen, R., Meleshko, V., Mugara, R., Palmer, T., Pierrehumbert, R., Sellers, P. & Trenberth, K. 2001 *IPCC, 2001: Climate Change 2001: the Scientific Basis. Contribution of Working Group I to the Third Assessment Report of the IPCC*. Cambridge University Press, Cambridge, UK, pp. 417–470.

Sun, F., Roderick, M. L., Lim, W. H. & Farquhar, G. D. 2011 Hydroclimatic projections for the Murray-Darling Basin based on an ensemble derived from Intergovernmental Panel on Climate Change AR4 climate models. *Water Resour. Res.* **47**, 1–14.

Tan, M. L., Ibrahim, A. L., Yusop, Z., Duan, Z. & Ling, L. 2015 Impacts of land-use and climate variability on hydrological components in the Johor River basin, Malaysia. *Hydrological Sciences Journal* **60** (5), 873–889.

Wang, R., Kalin, L., Kuang, W. & Tian, H. 2014 Individual and combined effects of land use/cover and climate change on Wolf Bay watershed streamflow in southern Alabama. *Hydrol. Process.* **28**, 5530–5546.

Wilby, R. L., Hay, L. E., Gutowski Jr, W. J., Arritt, R. W., Takle, E. S., Pan, Z., Leavesley, G. H. & Clark, M. P. 2000 Hydrological responses to dynamically and statistically downscaled climate model output. *Geophys. Res. Lett.* **27**, 1199–1202.

Wisal, K., Asif, K., Ullah, K. A. & Mujahid, K. 2020 Evaluation of hydrological modeling using climatic station and gridded precipitation dataset. *MAUSAM* **71** (4), 717–728.

Worku, G., Teferi, E., Bantider, A. & Dile, Y. T. 2020 Statistical bias correction of regional climate model simulations for climate change projection in the Jemma sub-basin, upper Blue Nile Basin of Ethiopia. *Theor. Appl. Climatol.* **139**, 1569–1588.

Wu, Y., Liu, S., Sohl, T. L. & Young, C. J. 2013 Projecting the land cover change and its environmental impacts in the Cedar River Basin in the Midwestern United States. *Environ. Res. Lett.* **8** (2), 024025.

Yi, L. & Sophocleous, M. 2011 Two-way coupling of unsaturated-saturated flow by integrating the SWAT and MODFLOW models with application in an irrigation district in arid region of West China. *J. Arid. Land.* **3**, 164–173.

Yu, W., Zhao, Y., Nan, Z. & Li, S. 2013 Improvement of snowmelt implementation in the SWAT hydrologic model. *Acta Ecol. Sin.* **33**, 6992–7001.

Zhang, L., Karthikeyan, R., Bai, Z. & Srinivasan, R. 2017 Analysis of streamflow responses to climate variability and land use change in the Loess Plateau region of China. *Catena* **154**, 1–11.

First received 18 June 2021; accepted in revised form 11 October 2021. Available online 27 October 2021